DEVELOPMENT OF INTERMETALLIC COATINGS FOR FUSION POWER APPLICATIONS*

J.-H. Park, T. Domenico, G. Dragel, and R. Clark
Energy Technology Division
Argonne National Laboratory, Argonne, Illinois 60439

March 1994

Manuscript submitted for publication in the proceeding at The third International Symposium on Fusion Nuclear Technology, June 27-July 1, 1994, Los Angeles, CA

*This work has been supported by the U.S. Department of Energy, under Contract W-31-109-Eng-38.

DEVELOPMENT OF INTERMETALLIC COATINGS FOR FUSION POWER APPLICATIONS*

J.-H. Park, T. Domenico, G. Dragel, and R. Clark
Energy Technology Division
Argonne National Laboratory, Argonne, Illinois 60439

In the design of liquid–metal cooling systems, corrosion resistance of structural materials and magnetohydrodynamic (MHD) force and its subsequent influence on thermal hydraulics and corrosion are major concerns. The objective of this study is to develop stable corrosion-resistant electrical insulator coatings at the liquid-metal/structural-material interface, with emphasis on electrically insulating coatings that prevent adverse MHD-generated currents from passing through the structural walls.

Vanadium and V-base alloys (V-Ti or V-Ti-Cr) are potential materials for structural applications in a fusion reactor. Insulator coatings inside the tubing are required when the system is cooled by liquid metals. Various intermetallic films were produced on V, V–5Ti, and V–20 Ti, V–5Cr-5Ti and V–15Cr–5Ti, and Ti, and Types 304 and 316 stainless steel. The intermetallic layers were developed by exposure of the materials to liquid lithium of 3–5 at.% and containing dissolved metallic solutes (e.g., Al, Be, Mg, Si, Ca, Pt, and Cr) at temperatures of 416-880°C. Subsequently, electrical insulator coatings were produced by reaction of the reactive layers with dissolved nitrogen in liquid lithium or by air oxidation under controlled conditions at 600-1000°C. These reactions converted the intermetallic layers to electrically insulating oxide/nitride or oxy-nitride layers.

This coating method could be applied to a commercial product. The liquid metal can be used over and over because only the solutes are consumed within the liquid metal. The technique can be applied to various shapes (e.g., inside/outside of tubes, complex geometrical shapes) because the coating is formed by liquid-phase reaction.

This paper will discuss initial results on the nature of the coatings (composition, thickness, adhesion, surface coverage) and their in-situ electrical resistivity characteristics in liquid lithium at high temperatures.

---

*This work has been supported by the U.S. Department of Energy, under Contract W-31-109-Eng-38.

1. Introduction

Corrosion resistance of structural materials and magnetohydrodynamic (MHD) force and its influence on thermal hydraulics are major concerns in the design of liquid–metal cooling systems.[1-3] The objective of this study is to develop in situ stable corrosion–resistant coatings as well as insulator coatings at the liquid-metal/structural-material interface. The electrically insulating coatings should be capable of forming on various shapes such as the inside of tubes or irregular shapes during operational conditions to prevent adverse currents that are generated by MHD forces from passing through the structural walls. The coatings could also improve general corrosion resistance and act as a diffusion barrier for hydrogen isotopes, viz., deuterium and tritium.

In this paper, three steps have been demonstrated for the fabrication of electrical insulator coatings applied to the liquid-lithium environment, i.e., (1) screening test for the candidate ceramic materials in liquid-Li environments, (2) in-situ fabrication of intermetallic or ceramic coatings in liquid-Li on the desired structure materials, and (3) in-situ electrical resistance of insulator coatings on V-5%Cr-5%Ti as a function of time and temperature in Li environments. Thermal cycling was conducted to investigate the integrity of the coating layers that formed in situ.

2. Compatibility Test of Electrical Insulators

Several insulators have been verified as compatible insulators in liquid-Li tests as shown in table 1. The test conditions and materials are listed. Table 1 collected the experimental results tested in the flowing liquid-Li. The trend for the liquid-Li compatibility for the tested ceramic insulators was followed by the thermodynamic criterion. Although some ceramic materials are fall in the category of thermodynamically stable materials, e.g., sintered AlN and CVD-SiC, they were not compatible with liquid-Li screening test. We could conclude that caused by the impurity incorporation in the grain-boundaries which could be reactive with liquid-Li, such as enriched oxygen, silicon, or carbon in AlN, SiC, etc. One of the example is sintered AlN. EDS analysis indicated that oxygen contamination was predominant in AlN. Those oxygen may form Al_2O_3 near the grain-boundary area which is not stable oxide in the liquid-Li environment. It reacted with lithium near the boundaries, that weakening the mechanical strength for the substrate AlN. As a result, oxygen enriched AlN become brittle after exposure in liquid-Li. When the impurity oxygen become

gathered into the Y/Y_2O_3 phase present in the AlN, the sintered AlN become intact in the liquid-Li environments. This presumably indicates that the both phases of AlN and Y_2O_3 are all compatible ceramics as we see in table-1. Based on the results of the liquid-Li compatibility tests we could realize the in-situ coating method for the given condition could be eliminates the difficult problems to serve in the liquid-Li environments. Therefore, this study has been focused in-situ forming intermetallic and ceramic insulators in liquid-Li environments.

Table 1. Liquid-Li compatibility of the insulator material in Li.

Identity	Composition	Vendor	*a / *b	Observation
SiC	SiC (CVD)	Northern	1/1	Reacted
	SiC (Si-enriched)	Northern	1/1	Reacted-heavily
	SiC (Hot Pressed)	Northern	3/1	Intact
Si_3N_4	Si_3N_4 (Hot Pressed)	Northern	0/1	Specimen not recovered
	Si-N-O (IBAD-coating)	ANL	0/1	Coating layer totally dissolved
Quartz	SiO_2 (Quartz Tube)		0/1and 2	Specimen not recovered
Rutile	TiO_2 (Single Crystal)		0/1	Specimen not recovered
Ytrria	Y_2O_3 (Sintered)	Ceres	3/1	Intact
	Y_2O_3 (Hot-Pressed)	ANL	3/1	Intact
YSZ	ZrO_2-10%Y_2O_3			
	Sintered	Coors	1/1	Reacted heavily
	Single Crystal	Ceres	1/1	Reacted heavely
Chromia	Cr_2O_3 (Hot Pressed)	ANL	0/1	Specimen not recovered
AlN	AlN	ORNL	3/2	Intact[4]
	AlN*c (1-3% Y incorporated)	ANL	3/1	Intact
	AlN (Sintered -oxygen enriched)	ANL	2/1	Reacted
	Al(V)N or AlN Al-O-C-N	ANL	3/2	AlN, Al(V)N, or Al-O-C-N formed in-situ in liquid-Li on V-5Cr-5Ti

BN	BN (Hexagonal)	Northern	0/1	Specimen not recovered
	BN (IBAD coating)	ANL	0/1	Coating totally dissolved
Si	Single crystal	ANL	0/1	Specimen not recovered
Al_2O_3	Al_2O_3 (AD 998-sintered)	Coors	0/1	Specimen not recovered
d*TiN	e*TiN pure and doped (Si, Mg, Al, and O)	ANL	3/2	TiN formed on Ti in liquid-Li at T>650°C
CaO	CaO	ANL	3/2	T = 700°C, 266 hrs CaO formed on V-15Cr-5Ti*f
	CaO or Ca(V)O	ANL	3/2	T = 416°C, CaO or Ca(V)O formed in-situ in liquid-Li on V-5Cr-5Ti*f
MgO	MgO	B&W	3/2	Intact[4]
	MgO	ORNL	3/2	Intact[4]
	MgO or Mg(V)O	ANL	3/2	416°C, CaO or Ca(V)O formed in-situ in liquid-Li on V-5Cr-5Ti
BeO	BeO	General Ceramics	3/2	Intact[4]
	BeO	Coors	3/2	Intact[4]
	BeO or Be(V)O	ANL	3/1 and 2	416°C, BeO or Be(V)O formed in-situ in liquid-Li on V-5Cr-5Ti
Yttrium-aluminum garnet	$Y_3Al_2O_{12}$	Union Carbide	3/2	Intact[4]

*a Score for liquid-Li compativbility: 0 indicates not compatible and 3 denotes compatible.

*b Method 1= flow: Liquid-Li compatibility of the insulator material in flowing Li test at 450°C (time between 315 to 617 hours), and Method 2 = capsule: Liquid-Li compatibility of the insulator material in Li test in capsule at 400°C for 100 hours *c ICP-Spectrochemical analysis for AlN samples shows the impurity level in (wt.%), As <0.05, Ba = 0.005, Be <0.001, Ca = 0.54, Co <0.002, Cr <0.002, Cu = 0.006, Fe = 0.015, Y = 3.77, Y_2O_3 = 4.79, Mg = 0.004, Mn < 0.001, Ni = 0.002, Pb < 0.02, Sb < 0.05, Sn <0.02, Sr <0.001, Ti = 0.022, V <0.002, Zn <0.002, Zr < 0.002, and Te <0.05. Before and fter the test, only the Li were analysed again. The Li contents were, <0.01 and 6.85, respectively. *dTiN is an electrical conductor. *e Type 304/316 container bearing Li + N. *f Li + Ca used for this studies.

3. Intermetallic and Ceramic Coatings in In-Situ in liquid-Li

Vanadium and V-base alloys (V-Ti or V-Ti-Cr) are proposed as the potential materials for structural applications in a fusion reactors. [5] Current studies have been focused on V and its alloys. Insulator coatings inside the tubing are required when the system is cooled by liquid metals. When the dissolved metallic solutes can be formed in a stable intermetallic phase with substrates in the liquid-Li environments, it is useful to fabricate the various intermetallic coatings for the desired stable insulators in the liquid-Li. Various intermetallic layers were developed by exposure of the materials to liquid lithium containing dissolved metallic solutes (e.g., Al, Be, Mg, Si, Ca, Pt, and Cr). Subsequently, electrical insulator coatings were produced by reaction of the reactive layers with dissolved oxygen or nitrogen in liquid lithium or by gas phase oxidation under controlled conditions. Intermetallic coatings that form on structural alloys during exposure to liquid Li containing dissolved metallic solutes suggest a means for producing stable electrical insulator layers by subsequent oxidation or nitridation of the intermetallic layer in the liquid–metal environment, as we proposed previously. [6] Several intermetallic coatings were produced on the vanadium and V-alloys and stainless steels.

3.1. Aluminide Coatings

Aluminide coatings that form on structural alloys during exposure to liquid Li that contain dissolved Al suggest a means for producing stable electrical insulator layers, such as AlN, by subsequent nitridation of the intermetallic layer in the liquid–metal environment. [6] The formation of several aluminides (V_xAl_y) that contain >40–50 at.% of Al on V–base alloys can be predicted from the V-Al phase diagram. [7,8] The Al-Li phase diagram indicates that Al is soluble in liquid Li, whereas V is not soluble in Li. [8] These phase relations make up the underlying basis for the formation of aluminide coatings on V and its alloys in liquid Li. Aluminide coatings were produced on V and V–base alloys by exposure of the materials to liquid Li that contained 3–5 at.% Al in sealed V and V-20%Ti capsules. [6] The nature of aluminide coatings formed on V, Ti, and V–base alloys containing Ti and Cr at 775–880°C. Various intermetallic or ceramic films were produced on V, V–5Ti, and V–20Ti, V–5Cr-5Ti and V–15Cr–5Ti, and Ti. Aluminide coatings were produced on V, Ti, and several V–base alloys (V-5%Ti, V-20%Ti, V-5%Cr-5%Ti, and V-15%Cr-5%Ti) by exposure of the materials to liquid Li

containing Al at temperatures of 775, 800, 860, and 880°C and Types 304 and 316 stainless steel at 650°C and above temperatures. The specimens and liquid Li were contained in V-20%Ti and V or stain less steel capsules that were placed in a larger stainless steel container. An argon cover gas (99.999% pure) was maintained in the system to prevent oxidation of the V capsules and the Li. The whole assembly was placed in a vertical furnace. At the end of the test, the capsules were cut open above the Li level to remove the samples. The capsules were placed in a beaker of water to dissolve the small volume of Li and the samples were removed and cleaned ultrasonically in acetone and ethanol and dried in air. The samples were examined by optical microscopy and SEM, and analyzed by EDS and X-ray diffraction. Hardness of the coating layers and bulk alloys was determined by Vickers indentation measurements with a Leitz microhardness tester. Degree of surface coverage and thickness of the layers varied considerably, depending on exposure time and temperature. At temperatures and exposure times of <800°C and <90 h, respectively, the aluminide layers were not uniform. Figure 1 shows the microstructures of aluminide coatings formed at 775°C for 87 h and 880°C for 48 h. At the lower temperature, small grains on the surface began to connect with neighboring grains by a grain–growth mechanism. At the higher temperature, the microstructure reveals that grain size is larger by at least one order of magnitude. Dependence of Al concentration at the coating surface on temperature is shown for several samples in Fig. 2. The EDS analysis of the coating surface was obtained over a region of 1,000 x 1,000 μm.

Figure 1. Typical aluminide surface formed on V-5%Cr-5%Ti at 775 and 880°C

A typical cross section of an aluminide coating layer is virtually defect–free, but an array of small defects is present beneath the compact layer. These defects may be

clustered near a dislocation zone that is depleted in Al and rich in Li because of fast diffusion of Li via dislocations. Composition–vs.–depth profiles for the V and V-20%Ti specimens are shown in Fig. 3. The depth of Al interdiffusion in V-20%Ti is ≈3-4 times greater than in pure V at 860°C, which suggests a higher mobility of Al in V-20% Ti than in V.

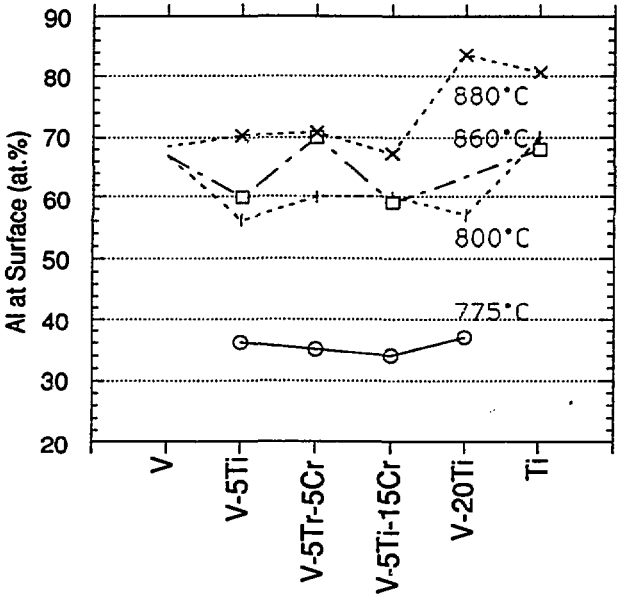

Figure 2. Aluminum content of aluminized surfaces formed on several V–base alloys and Ti at several temperatures between 775 and 880°C

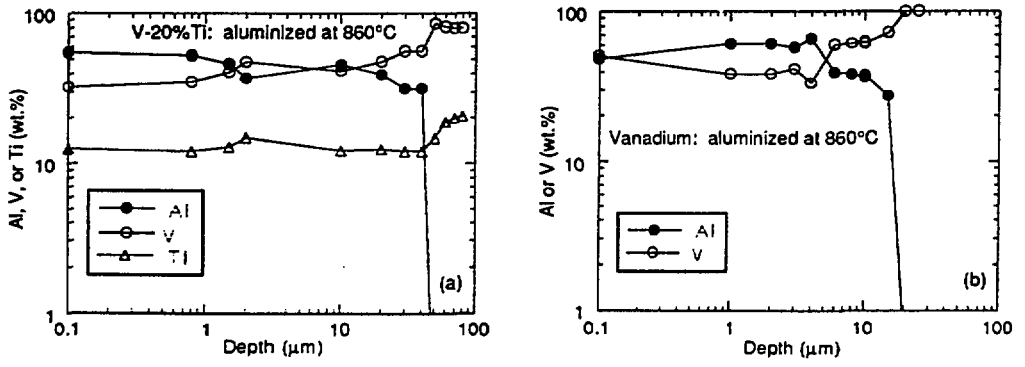

Figure 3. Chemical composition as a function of depth for aluminide layers on (a) V-20%Ti and (b) V

Vickers hardness measurements of the aluminide layers and the underlying V and V-20%Ti alloy were conducted at 25– and 50–g loads. The aluminide layers were harder than either V or V-20%Ti, which can be attributed to interstitial Al atoms in the cubic lattice of V. Because the distribution on nonmetallic elements (O, N, C, H) between V–base alloys and Li favors the Li, the alloys tend to become depleted in these constituents during exposure to high–temperature Li. Consequently, the hardness increase is most likely caused by diffusion of Al into V and V–20%Ti. Our experience indicates that V becomes more ductile after exposure to liquid Li.

Figure 4 illustrates the high degree of coverage of an aluminide layer on a weld joint between a V–20%Ti tube and a V disk, as well as in the crevice region where fusion did not occur. Figure 4a shows a cross section of the capsule containing the weld zone; it reveals shallow penetration and a crevice between the tube and the disc. Figure 4b shows this region in higher magnification. The aluminide coating is not only present on the surface of the tube and the face of the disk, but also penetrates the 1–μm space between the V-20%Ti tube and V disk. The thickness of the coating in this region is similar to that on the inner surface of the tube and the disk exposed to liquid Li. Figure 4c shows that the gap region between tube and the edge of the disk (denoted by the arrow in Fig. 4a) has also been coated. The coating behavior suggests that bulk diffusion is the main process. Conversion of aluminide layers to an electrical insulator coating (e.g., an AlN film) in liquid-Li has been conducted.

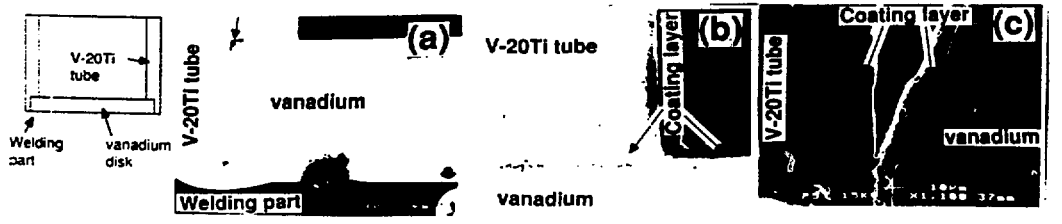

Figure 4. (a) Cross section of weld zone between V–20%Ti tube and V disk, (b) aluminide coating on surface of tube and disk and in crevice region between tube and disk, and (c) coating of gap region between tube and disk, denoted be arrow in (a)

3. 2. AlN Coating on Aluminide V-5%Cr-5%Ti

AlN Coating in High N concentration: The aluminide layer was then nitrided in an Li–Li_3N mixture (≈ 3-5 at.% N) in a system that also allowed measurement of electrical conductivity during formation of the AlN layer. Figure 5 shows the results of the in-situ ohmic resistance on temperature over the duration of the experiment. The coating area (surface of the tube in contact with liquid Li) was 20 cm^2. If we assume that the thickness of the AlN film is ≈1 μm, the electrical conductivity at 700°C is consistent with literature values. [9] However, thermal cycling tends to decrease the resistivity, as shown in Fig. 5 for the second cycle. Ohmic resistance dropped from ≈1.5 to 0.43 Ω and remained constant after the temperature was increased to 800°C, where we expected that the reaction between the aluminide layer and N would proceed at a higher rate and thereby show an increase in resistance over the previous value of ≈1.5 Ω. This trend, if it had occurred, would indicate that nitriding of spalled regions or defects (e.g., cracks or open boundaries) in the film occurs rapidly.

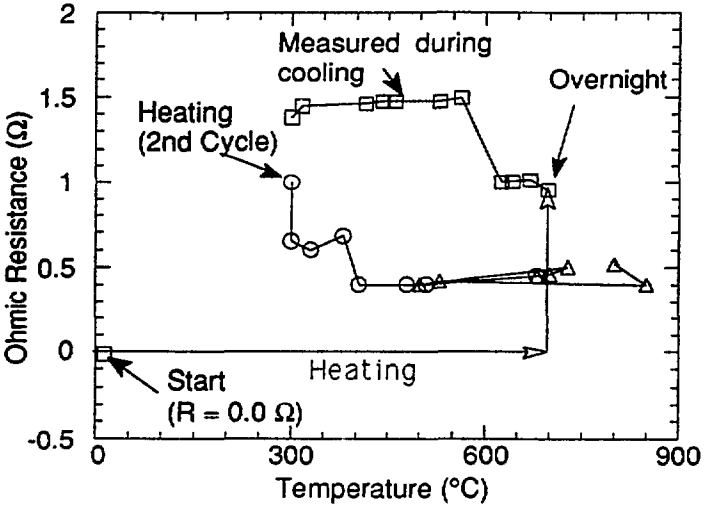

Figure 5. Ohmic resistance vs. temperature during heating cycles.

Figure 6 shows SEM micrographs of an AlN film and a spalled area on an aluminide surface of V–20%Ti, along with electron–energy–dispersive–spectroscopy (EDS) spectra from the two regions. The EDS results indicate a relatively high concentration of Al, N, and O in the coating compared to the spalled area. Electrical resistivity of the

AlN film was measured at room temperature after the cell was dissembled. The ohmic resistance was $>10^{12}$ Ω. which indicates that it is a good electrical insulator.

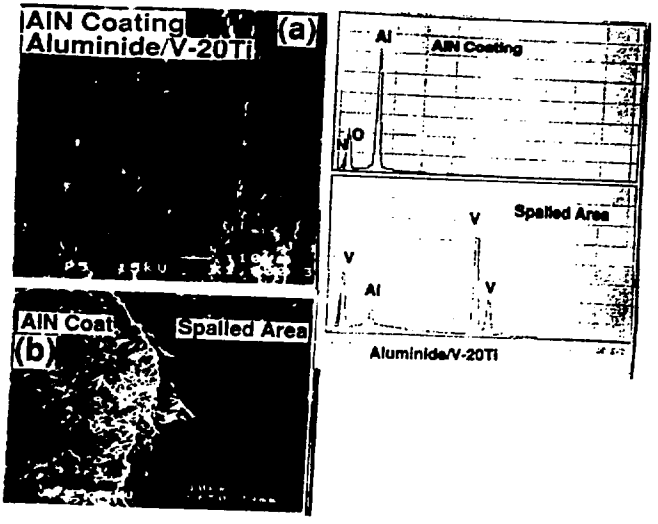

Figure 6. (a) SEM micrograph of surface of AlN on aluminide layer on V-20%Ti, (b) AlN and spalled area of coating, and (c) EDS spectra from AlN layer and spalled area in (b).

Aluminide V-5Cr-5Ti Exposure in 100 ppm N in liquid-Li : The pre-aluminide V-5%Cr-5%Ti samples were exposed in liquid-Li containing 100-150 ppm nitrogen at 410°C and 500°C for 672 hours to examine the formation of nitride layers. Tests were performed with monitoring the electrical resistance with time. In the tests, the ohmic values were developed 0.01 to 0.18 Ω during the period. However, the microstructure and the composition of the aluminide layers were changed as shown in figure-7.

Table 2. Liquid-Li compatibility for aluminides coatings on V-alloys.

Samples	Exposure T(°C)	Exposure Time (h)	Comments
Aluminide/304SS	450	315	Al kept at surface
Aluminide/V-20Ti	450	315	Al kept at surface

Aluminide V-5Cr-5Ti	410	672	Al kept at surface Microstructure changed, grain-size, 2-3 μm Ti enriched near the surface especially in grainboundary
V-5Cr-5Ti (without coating)	410	672	grain-boundary revealed
Aluminide/ V-5Cr-5Ti	500	672	Al kept at surface Microstructure changed, grain-size, 3-4 μm Ti enriched near the surface especially in grainboundary
V-5Cr-5Ti (without coating)	500	672	grain-boundary revealed more coarsened than 410°C

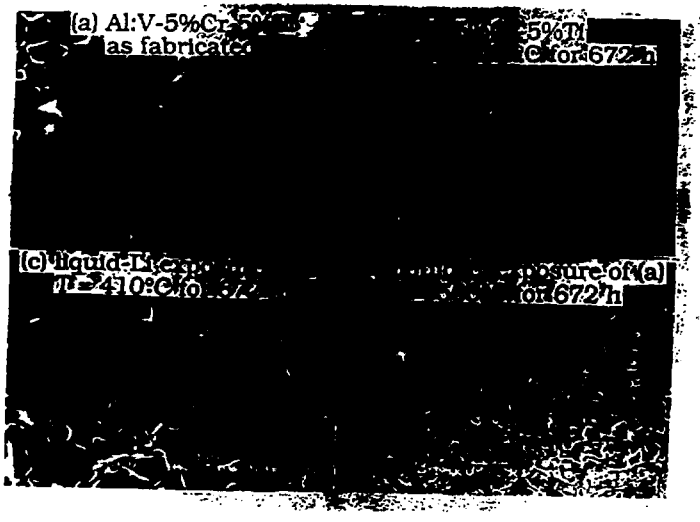

Fig. 7. Surface micro structures of (a) as aluminide surface on V-5%Cr-5%Ti at 880°C for 64 hours. Exposed for 672 hours in liquid-Li: (b) without coating sample , and (c) coated shown (a) at 410°C and (d) 500°C.

Figure 7 shows the microstructures of aluminide V-5%Cr-5%Ti and exposed in liquid-Li at 410°C and 500°C. Samples (2.75 " long x 0.25 " wide x 0.05 " thick) were used for this tests to see the differences of microstructures between exposed in the vapor phase and in liquid-Li phase. At the vapor phase did not changed the micro structures for both temperatures tested. But in the liquid-Li phase we see the variation of micro structures between as fabricated and exposed in liquid-Li as shown in fig. 7. According to the EDS analysis, the different shape of grain shows different chemical compositions as shown in fig 8. Mainly the Ti become enriched at the sample surfaces. This trend may be accounted in terms of thermodynamic stability of TiN has highest stability in the condition as we shown in table 1. In those situation, TiN become enriched at the surface for the long time operation.

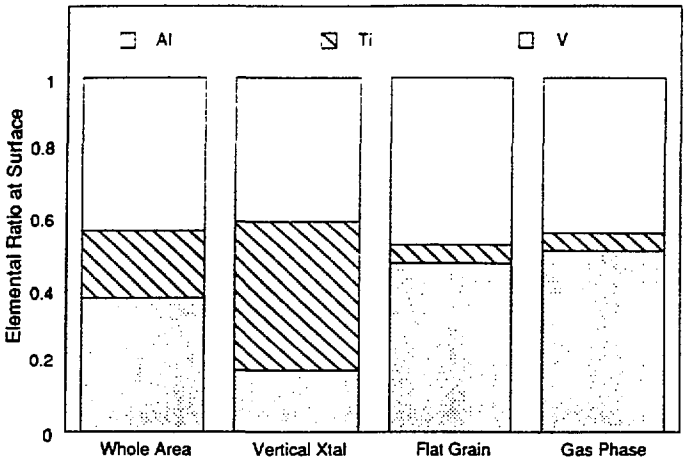

Fig. 8.
Element ratio for the exposed (in liquid-Li) and unexposed (in Ar with vapor-Li: gas phase) aluminide coating on V-5%Cr-5%Ti surface.

From the results of these tests, we could conclude that the Ti become enriched at the surface based on the morphology. As we generally predicted that the AlN could be formed in the nitrogen concentration of 150 ppm in liquid-Li environment, but in the layer Ti become enriched by the thermodynamic driving force. As a result, the localized V-Al-Ti-N which is conductive layers become developed in the 100-150ppm N environments. Therefore, pre-aluminide procedure in the V-alloys system may not be obtained high enough ohmic resistance in the low nitrogen atmosphere even though AlN is thermodynamically stable, the V-Ti-Al-N phase being formed due to the outward diffusion of more stable nitride forming V or Ti via nitride layers in the low nitrogen concentration.

3. 3. Nitride Coating on un-aluminide V-5%Cr-5%Ti

The electrical resistance of insulator coatings produced on un-aluminide V-5%Cr-5%Ti by exposure of the alloy to liquid Li that contained 5 at.% N, with and without 5 at.% dissolved Al, was measured as a function of time at temperatures between 250 and 500°C. The solute elements (N and Al) reacted in liquid Li with the alloy substrate at 415°C to produce thin adherent coatings. The resistance of the coating layer was ~1.5 and 1.0 ohm at 415 and 500°C, respectively. Thermal cycling between 250 and 415°C did not change the resistance of the coating layers. These results and those reported previously suggest that thin homogeneous coatings can be produced on various shaped surfaces by controlling the exposure time, temperature,

and composition of the liquid metal. The integrity of the coatings does not appear to sensitive to defects (e.g., open pores, fissures, or microcracks) present in the alloy substrate in liquid Li. We could predict the self-healing profile by monitoring the resistance versus time in a in-situ liquid-Li. At 416°C shows parabolic shape of self-healing was in the rate of 0.04 Ω/√h.

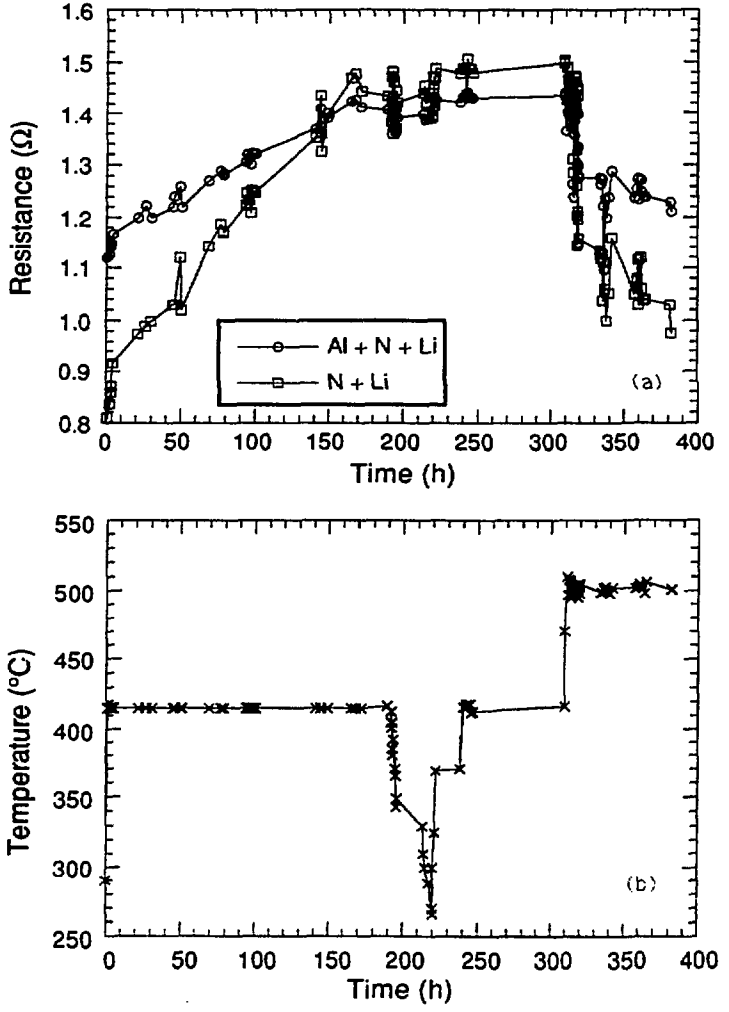

Figure 9. (a) Electrical resistance of V–5%Cr–5%Ti in Li containing N and Al (Cell A) and N (Cell B) and (b) temperature versus time of exposure in the liquid Li environments

The test conditions and results from the in-situ electrical resistance of 150 mm^2 of V-5%Cr-5%Ti in contact with liquid Li are given in Fig. 9. Initially, Cell A exhibited higher ohmic values than did Cell B up to 150 h, but the ohmic values of both cells were almost identical thereafter. During thermal cycling between 415 and 250°C the changes in resistance were small. This result presumably indicates that the layers did not show any degradation such as spallation or local defects. When the temperature was increased from 415 to 500°C, the ohmic resistance dropped from ≈1.4 to 1.0 Ω for Cell A, and from ≈1.5 to 0.95 Ω for Cell B.

The decrease in resistance could be attributed to the temperature dependence of the electrical resistivity of the coatings, i.e., the equilibrium composition of ionic and electronic species varies as a function of temperature, whereas normally, more defects are expected at higher temperatures. Thus, more electronic mobile carriers could form and act as charge-compensating defects at higher temperatures. Alternatively, as the temperature was increased, the level of Li in the capsule rose owing to thermal expansion. Consequently, additional alloy surface was exposed to the liquid. As shown in Fig. 9, at 500°C the resistance of both cells returned to their initial values at 415°C, which may indicate that a fully developed coating was not present on the alloy surface above the original liquid/gas interface. During the last ≈80 h of the test, the resistance of the film did not increase as expected because of possible N depletion in the liquid due to reaction with the surface of the aluminized capsule (150 mm^2) that was in contact with liquid Li and to loss of N to the gas phase.

In principle, the time variation of electrical resistance at 500°C can provide kinetic information on the reequilibration process; Cell A showed slower kinetics than did Cell B, which can be expected because the thin layer of AlN on Cell A presumably is more insulating.

Questions remain on the details of the kinetics of reactions that describe in-situ formation of an insulator coating in liquid Li environments. [10] Throughout the experiment, a high–purity Ar cover gas was present and no attempt was made to maintain N_2 in the gas phase. Because the cells could not be sealed, loss of N to the gas phase probably occurred, which could influence in-situ formation or rehealing of the coating layer under conditions of the experiment. However, had the alloy surface been in direct contact with the liquid because of partial spallation or cracking of the insulator layer without healing, the ohmic resistance would decrease to zero (i.e., short circuit by metallic contact). Neither of the cells exhibited short–circuit behavior during the 400–h experiment.

Insulator coatings formed in situ on V-5%Cr-5%Ti in liquid Li that contained Li_3N, with and without dissolved Al, at 415°C. The ohmic resistance of the coatings was ≈1.0 —1.5 Ω. Thermal cycling between 415 and 250°C did not produce changes in the resistance of the coatings.

3.4. Al_2O_3 Coating on Stainless Steels

Al_2O_3 electrical insulator coatings were produced by air oxidation at 1000°C. These reactions converted the intermetallic layers to electrically insulating oxide layers around the Types of 304 and 316 stainless steel tube inside without spallation which may not be easy to achieved with other method. [5] The dissolved ≈100 ppm of Li during aluminide process in the stainless steel helped the stabilization of Al_2O_3 coating layers during oxidation. Al_2O_3 coating layers were shown very good insulator at ambient temperatures. Further tests were not conducted in liquid-Li exposure due to the previous results indicates incompatible in liquid-Li environments [13] and shown in Table-1.

3.5. Be Coating on V-5Cr-5Ti

Beryllium and many important metals are well forming the Be-intermetallic phases including V, such as, Ba, C, Ca, Co, Cr, Cu, Fe, Hf, Ir, Mg, Mn, Mo, N, Nb, Ni, O, Po, Pt, Pu, Re, Rh, Ru, Sb, Sc, Se, Sr, Ta, Th, Ti, U, W, Y. Yb, and Zr. These information directly implied into the V-5%Cr-5%Ti or any V-Cr-Ti alloys are subjected to making an useful Be-(V, Cr, Ti) intermetallic coatings on the alloys. Beryllium intermetallic coating that form on structural alloys during exposure to liquid lithium containing dissolved Be suggest a means for producing stable electrical insulator layers, such as BeO, Be_3N_2, or Be-O-N by subsequent oxidation, nitridation of the intermetallic layer in the liquid metal environment. According to the Be-V binary phase diagram, $Be_{12}V$ and Be_2V intermetallic phases are reported shown in Fig. 10. Be-V intermetallic coatings that form on structural alloys during exposure to liquid lithium containing dissolved Be suggest a means for producing stable Be-V phase(s) which could be on the V-5%Cr-5%Ti of the intermetallic layer in the liquid metal environment. As well for Cr, the $CrBe_2$ and $CrBe_{12}$, and for the Ti, the $TiBe_2$, $TiBe_3$, Ti_2Be_{17}, and $TiBe_{12}$, these provide the all the components in the V-5%Cr-5%Ti are subjected to stabilized by the intermetallic phases with Be. These intermetallic phases

could be formed in the Fe-Cr based structure alloys and they also could be applied in-situ coating works in the liquid-Li environments. Figure-10 shows the Be-V intermetallic phase of Be_2V coated on the V-5Cr-5Ti surface and a depth profiling obtained by secondary ion mass spectroscopy.

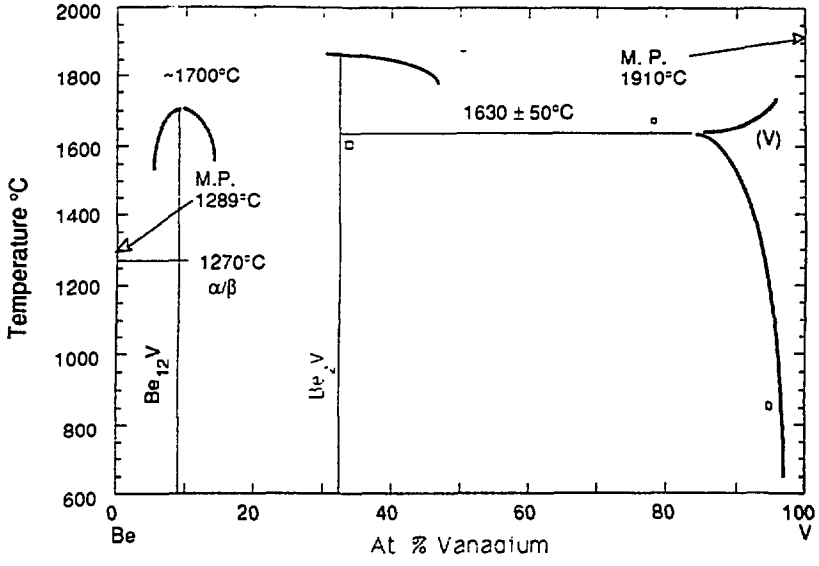

Fig. 10. Phase diagram of binary Be-V.

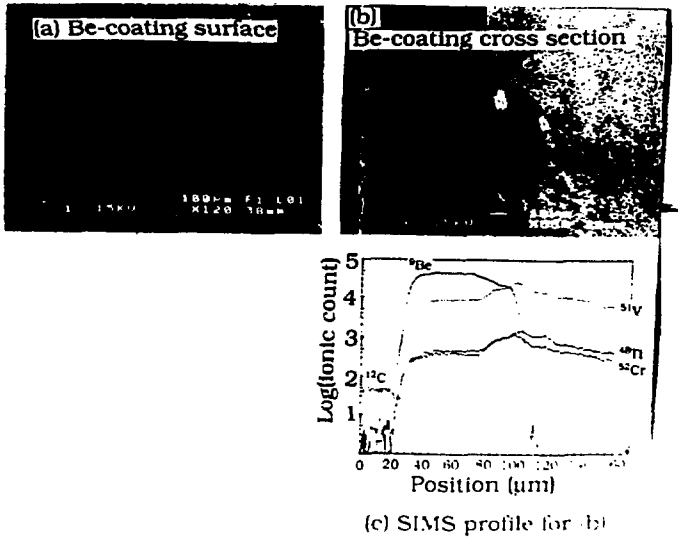

(c) SIMS profile for (b)

Figure 11. Be-V intermetallic phase of Be_2V coated on the V-5Cr-5Ti surface(a), cross section (b), and a depth profiling obtained by secondary ion mass spectroscopy (c).

3.6. TiN Coating

TiN is well known electronic conduction ceramic material, and thermodynamically stable nitride in liquid-Li. A similar fabrication approach was adapted as shown in AlN coating works. Sample of pure Ti and a pair of Ti electrodes were placed in small capsules containing liquid Li and Li_3N for seven days at 710°C to investigate the formation of titanium nitride (TiN). An attempt was made to enhance the resistivity of in–situ–formed TiN films by adding to the Li small amounts of Al, Si, and Mg, which might be incorporated into the films. One sample and set of electrodes was nitrided in Li containing Li_3N and another was immersed in pure Li. The electrical resistance of the films was ≈1.0–1.5 Ω and the values increased slightly with temperature, which is indicative of metallic conduction. [11]

3.7. CaO Coating

In the case of useful metallic solutes do not make intermetallic phases with vanadium or its alloys, such as Ca or Mg, a similar fabrication approach could be adapted as shown in-situ intermetallic coating works with charging of oxygen or nitrogen (as a reactant) in the interstitial sublattice in the BCC (body-centered-cubic) lattice of vanadium and its alloys. [12] Initially, samples of V-5Cr-5Ti were heat treated in the flowing gases of nitrogen or argon at temperatures between 510 to 1030°C for the surface charging of oxygen or nitrogen. These oxygen or nitrogen reacted samples were dipped into the calcium bearing liquid-Li for four days at 420°C to investigate the formation of calcium oxide (CaO). Figure 12 shows the SEM micrograph of surface and cross section of CaO on V-5%Cr-5%Ti, and its EDS spectrum from CaO layer.

An attempt was made to enhance the resistivity of in–situ–formed CaO films by adding to the Li small amounts of Ca, which might be incorporated into the films. The electrical resistance of the films was ≈0.4– 3.5 Ω and the values decreased with temperature at below 650°C, which is indicative of predominates of ceramic insulator behavior, and the values decreased with temperature at above 650°C which is indicative of more or less metallic conduction. When the direct current supplied spontaneously through the electrodes, the polarization behavior was observed as high as the ohmic values increased at 539°C for 35.7 Ω for the 3 cm^2 area. This calculated value of 107 Ω cm^2 may be satisfied the required r times thickness (ρt), if the thickness

assumed 3 μm and based on the criterion of $\rho t \geq 25$—100 Ω cm^2 for the MFR applications. [13]

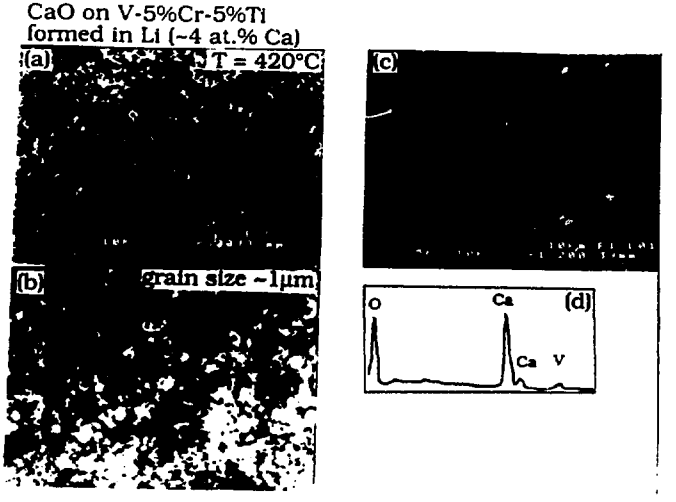

Figure 12. (a) SEM micrograph of surface of CaO layers on V-5%Cr-5%Ti, (b) shows the enlarged of (a), (c) the cross section view and (d) EDS spectrum from CaO layer.

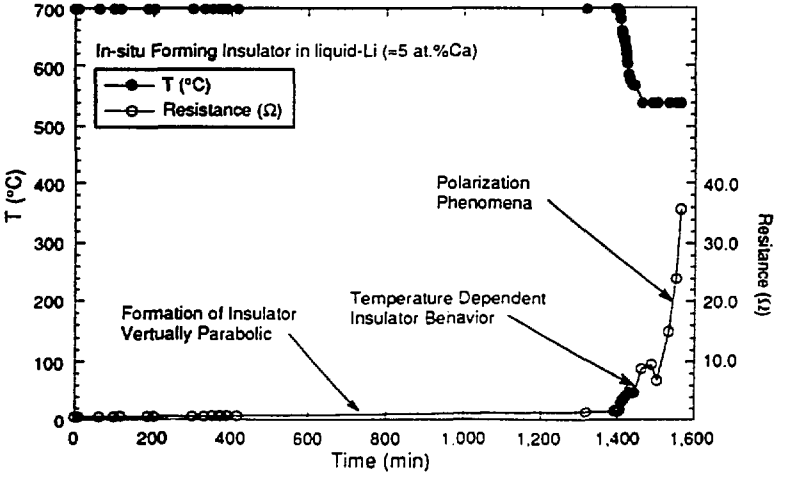

Figure 13. In-situ electrical resistance and liquid-Li temperature measurements as a function of time during fabrication of CaO coating in liquid-Li.

However, currently, the remaining problem which we can predict in Fig. 14. Two temperature cycling run showed the ohmic values abruptly drop at the two main drops at 500°C and 300°C for the first run, and 400°C for the second run. It has been scheduled to solve this problem for the extended temperature ranges from fabrication temperatures to freezinf temperature of liquid-metals, and down to room temperatures.

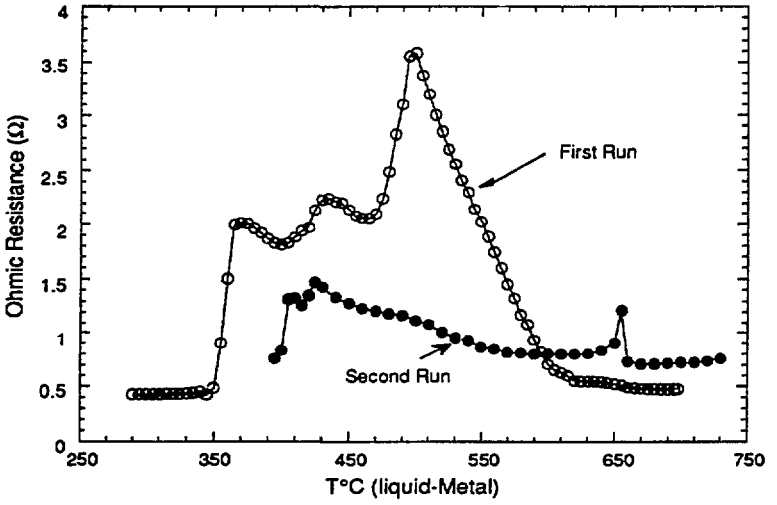

Figure 14. Ohmic values vs. liquid-Li temperature with cooling direction for the two different runs for the in-CaO layer in the V-5Cr-5Ti.

4. Thermodynamic Consideration for Coating Works

Nitride coatings (e.g., AlN, TiN, etc.) on aluminide layers and Ti can be produced in an Li + Li_3N mixture, based on thermodynamic considerations and the Li-Li_3N phase diagram. The melting points of Li and Li_3N are 180.6 and 815°C, respectively. The liqudus temperature increases monotonically as the nitrogen concentration increases. [14] However, an Li–Li_3N mixture at a given temperature provides a means of establishing a fixed nitrogen partial pressure that corresponds to the thermodynamic equilibrium for the two–phase mixture. Similarly, oxide (CaO and MgO) or nitride coating could be produced with or without intermetallic phases by charging the oxygen or nitrogen into the structure materials substrates. In this case dissolved solutes (e.g., Ca, Mg, or Al) in liquid-Li, and the let the chemical reaction take place at the surface by diffusing out the O or N from the substrates.

To rationalize the present conductivity measurements, the thermodynamic stability of several simple oxides and nitrides has been considered. Figure 14a shows calculated equilibrium partial pressures of O_2 and N_2 in the Li–Al–Y system as a function of temperature, [8] and Fig. 15b shows a schematic thermochemical diagram for the M-N-O system, where M denotes Al, Li, Ca and Y. In these experiments, it is difficult to exclude interactions with the gas–phase environment, especially O_2 contamination. When O_2 interacts with liquid Li and the O solubility limit is exceeded, Li_2O will form. Because Li_2O is the most stable oxide in the Li–Al–O system, it is not likely that Al_2O_3 will form. Similarly, an AlN layer is not likely to react with dissolved oxygen in Li to form Al_2O_3 because the latter is not stable in O–saturated Li. Consequently, AlN can be a stable phase in liquid Li with a relatively high N_2 partial pressure. Figure 15a indicates that the stability of AlN is greater than that of Li_3N over a wide temperature range.

Formation of an AlN film on an aluminide layer follows the reaction, $Li_3N + Al = 3\,Li + AlN$, where the free–energy change, ΔG, is –25 kcal/mole at 500°C. If the AlN film cracks or spalls, the reaction should take place and repair the film, provided that N is present in Li and the Al activity in the alloy is sufficient for spontaneous reaction to occur. The main requirement is that the N level in Li be high enough. If this is not the case, we must also consider the possibility of dissolution of the AlN film based on the solubility's of Al and N in liquid Li, i.e., AlN = $\underline{Al}$ + $\underline{N}$ (in Li).

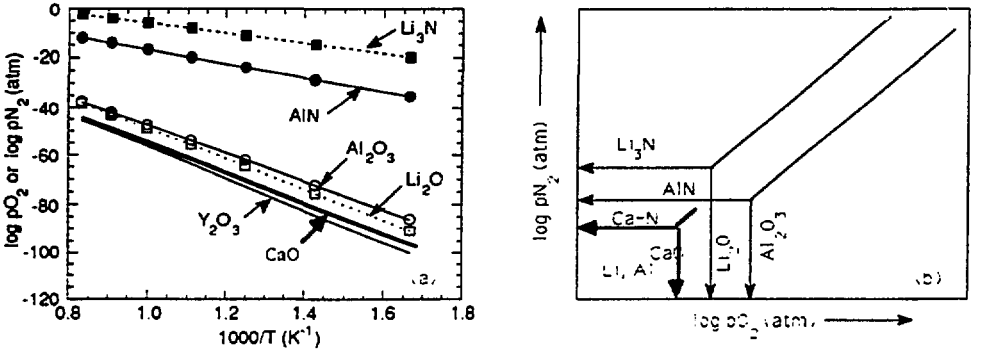

Figure 15. (a) Calculated equilibrium partial pressures of O_2 and N_2 in Li–Al–Y system and (b) schematic thermochemical diagram for M-N-O system, where M represents Al or Li

The ΔG for this reaction is +31.2 kcal/mole; therefore, the equilibrium constant K for the reaction at 500°C is $K = 2 \times 10^{-9} = a_{\underline{Al}} a_{\underline{N}}$, [15] when the activities for Li and AlN are assumed to be unity. The typical impurity level for N in Li is ≈50–200 ppm.

Therefore, the Al concentration in Li must be in the range of 10–40 ppm at 500°C to maintain the AlN layer. In capsule experiments, it is relatively easy to meet these criteria for the formation and long–term stability of the AlN phase. In a forced–circulation loop under heat transfer conditions, the effect of the temperature gradient throughout the system on the concentrations of Al and N in Li must be considered so that the AlN film can be maintained at all temperature regions over long periods of time. This will be explored in future work after additional information on the stability and resistivity of insulator coatings is obtained in capsule tests. For the CaO similarly considered, but thermodynamic stability of Ca-N or CaO are much higher than that of AlN, Li-N, or Li-O, it could be realized without detail analysis. Subsequently, the results will be applied to a flowing loop system for the application on the MFR system.

5. Conclusion

Based on the liquid-Li compatibility tests for insulator candidators, and the design works for the MFRs, the fabrication method for the insulator coating coatings were pursued as an in-situ in liqiud-Li environment. Surface modification via high-temperature liquid–phase deposition can provide intermetallic phase coatings on V–base alloys and Stainless steels. This process is facilitated in liquid Li because surface contamination by O_2 or oxide films is virtually eliminated, and the process to produce homogeneous coatings on various surface shapes can be controlled by exposure time, temperature, and composition of the liquid metal. Conversion of intermetallic or oxygen and nitrogen enriched layers to an electrically insulating coating (e.g., an AlN for the intermetallic coatings film and CaO for surface oxygen enriched samples) formed in liquid Li was demonstrated in the temperature range of 416°C to 880°C in liquid-Li environments. Especially, CaO layer was formed relatively easily in liquid-Li containing Ca even at 416°C. This study will be conducted to improve the mechanical stability to avoid the crack during thermal cycling and to find the mechanisms for the self-healing procedure.

Acknowledgement

The authors are thanks to Drs. D. L. Smith, R. Mattas, K. Natesan, and C. Reed for the support and review for the directions, and Dr. T. F. Kassner for the fruitful discussions and guidances especially in liquid-Li related experimental procedures during the works.

References

1. C. C. Baker et al., *Tokamak Power System Studies FY 1985*, Argonne National Laboratory Report ANL/FPP-85-2 (December 1985).
2. Y. Y. Liu and D. L. Smith, *Ceramic Electrical Insulators for Liquid Metal Blankets*, J. Nucl. Mater., **141-143**, 38 (1986).
3. T. Kammash, *Fusion Reactor Physics*, Chapter 15, Ann Arbor Science Pub. Inc., Ann Arbor, MI (1975) pp. 405-439.
4. R. J. Lauf and J. H. DeVan, Evaluation of Ceramic Insulator for Lithium Electrochemical Reduction Cells, J. Electrochem. Soc., 139, 2087-2091 (1992)
5. R. F. Mattas, B. A. Loomis, and D. L. Smith, *Vanadium Alloys for Fusion Reactor Applications*, JOM, **44**(8), 26 (1992).
6. J.-H. Park and G. Dragel, *Development of Aluminide Coatings on Vanadium–Base Alloys in Liquid Lithium*, Fusion Reactor Materials Semiannual Progress Report for the Period Ending March 31, 1993.
7. M. Hansen, *Constitution of Binary Alloys,* McGraw-Hill, New York (1958).
8. F. A. Shunk, *Constitution of Binary Alloys, Second Supplement,* McGraw-Hill, New York (1969).
9. S. F. Palguev, R. P. Lesunova, and L. S. Karenina, Solid State Ionics **20,** 255-258 (1986).
10. J.-H. Park and G. Dragel, *Development of Electrical-Insulator Coatings: In-situ Electrical Resistance Measurements on V-5%Cr-5%Ti in Liquid Lithium*, Fusion Reactor Materials Semiannual Progress Report for the Period Ending October 31, 1993.
11. J.-H. Park and T. Domenico, *Measurement of Electrical Resistivity of Thermally Grown Titanium Nitride Thin Film in Liquid Lithium*, Fusion Reactor Materials Semiannual Progress Report for the Period Ending October 31, 1993.
12. A. U. Seybolt and H. T. Sumsion, *Vanadium-Oxygen Solid Solutions,* J. Metals Trans. AIME 292-299 (1953).
13. B. F. Picologlou, Argonne National Laboratory, personal communication, 1991.
14. L. S. Darken and R. W. Gurry, *Physical Chemistry of Metals*, McGraw-Hill, New York (1953).
15. L. J. Wittenberg, Univ. Wisconsin, personal communication, 1993.